Abdominal Imaging

Published online: 9 December 2014

Abdom Imaging (2015) 40:745–759
DOI: 10.1007/s00261-014-0315-6

Magnetic resonance elastography of abdomen

Sudhakar Kundapur Venkatesh, Richard L. Ehman

Department of Radiology, Mayo Clinic, 200 First Street SW, Rochester, MN 55905, USA

Abstract

Many diseases cause substantial changes in the mechanical properties of tissue, and this provides motivation for developing methods to noninvasively assess the stiffness of tissue using imaging technology. Magnetic resonance elastography (MRE) has emerged as a versatile MRI-based technique, based on direct visualization of propagating shear waves in the tissues. The most established clinical application of MRE in the abdomen is in chronic liver disease. MRE is currently regarded as the most accurate noninvasive technique for detection and staging of liver fibrosis. Increasing experience and ongoing research is leading to exploration of applications in other abdominal organs. In this review article, the current use of MRE in liver disease and the potential future applications of this technology in other parts of the abdomen are surveyed.

Key words: Magnetic resonance elastography—Liver—Spleen—Kidney—Pancreas—Uterus—Liver fibrosis

Elastography

Mechanical properties of pathological tissues are often markedly different from those of normal tissues. With palpation, clinicians can evaluate the "stiffness" of tissues, and this technique is often used to detect tumors in accessible regions of the body such as the breast, thyroid, and prostate. Deeper structures, however, such as liver, spleen, and kidneys are much less accessible to palpation. Recognizing the potential diagnostic value of quantitatively evaluating the mechanical properties of tissue, several imaging-based "elastography" methods have been developed. The stiffness of human tissues (normal and abnormal) is spread over a wider range (several orders of magnitude) in contrast to other physical properties like X-ray attenuation coefficient, T1-relaxation, or bulk modulus (Fig. 1). The most commonly available quantitative elastography techniques currently used in clinical radiology are ultrasound-based shear wave elastography and MRI-based magnetic resonance elastography (MRE).

These dynamic elastography techniques exploit the fact that the propagation characteristics (such as speed) of shear waves depend on the mechanical properties of the medium. In dynamic shear wave elastography, shear waves are generated in tissue, and the resulting pattern of wave motion is assessed with ultrasound-based or MRI-based techniques. The measurements are then processed to determine the mechanical properties. Most human tissues are neither completely solid nor completely liquid and behave differently to stress compared to pure solids and liquids. In order to simplify the analysis, tissue is often assumed to be linear, viscoelastic, isotropic, and incompressible [1–3]. The elastic property assessed by palpation corresponds to what is expressed as Young's modulus (E), or shear modulus (μ). For most tissues, the Young's modulus and the shear modulus are related by a simple scale factor of $E = 3\mu$; therefore calculation of either modulus would give similar information termed tissue stiffness. When shear waves propagate through tissue, the shear stiffness of tissue can often be calculated to a good approximation from the measured shear wave speed (c) and the density of tissue (ρ) using the equation $\mu = \rho c^2$. Shear waves travel faster in stiffer tissues than in softer tissues, and this is reflected as longer wavelengths of the propagating shear waves and is easily appreciated in MRE-based wave images. More sophisticated mathematical techniques (sometimes called inversion algorithms) can allow estimation of the complex shear modulus, which reflects both the spring-like elastic property of tissue and a damping or viscous component and can yield images that represent these tissue mechanical properties and their spatial distribution. Images of tissue stiffness are often called elastograms or stiffness maps. Many review articles have provided detailed information on the technical basis of dynamic elastography [3–16].

Vibration-controlled transient elastography (TE), commercially known as Fibroscan [17, 18], is an

Correspondence to: Sudhakar Kundapur Venkatesh; *email:* venkatesh.sudhakar@mayo.edu

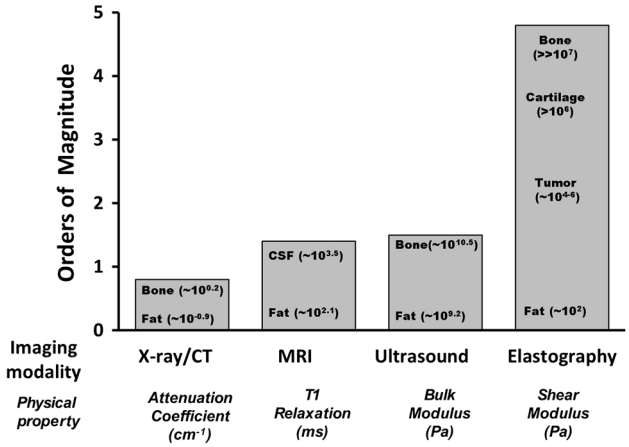

Fig. 1. Bar chart showing different imaging modalities and the spectrum of contrast mechanisms utilized by them are shown. The shear modulus has the largest variation (more than five orders) of magnitude among various physiological states of normal and pathologic tissues (adapted with permission from Mariappan et al. [15]).

ultrasound-based elastography technique that has been widely used to evaluate liver stiffness. With TE, an actuator in the ultrasound probe induces transient shear waves that propagate into the liver from the body wall. One-dimensional (1D) speckle tracking ultrasound is used to measure the speed of the wave as it propagates away from the transducer. TE typically assesses a volume of tissue in a 1×4 cm cylinder located about 25–65 mm from the skin surface. The measured shear wave speed is converted to an estimate of Young's modulus by the algorithm. TE is widely used especially in Asia and Europe and has shown excellent accuracy for distinguishing advanced fibrosis and cirrhosis from mild fibrosis and normal livers [19, 20]. TE has high interobserver agreement and is a reliable method for excluding cirrhosis [21]. Although TE is easy to perform, it has some limitations: it has limited success in obese patients and has a reported technical failure of 15%–20% of exams [21]. TE measurements are typically obtained at ten locations, but this is still a very small fraction of the volume of the liver and is confined to the periphery of the right lobe only. MRE performs better than TE in the detection and staging of mild fibrosis, especially significant fibrosis, which is considered as an indication to start anti-fibrotic therapy.

MRE has similarities to TE in that it is a dynamic elastography technique that generates shear waves and images the propagation of these waves in tissue. However, MRE has a key difference in that MRI permits 2D or 3D imaging of the propagating waves within the liver. This permits the system to create 2D or 3D images of elasticity, depicting and allowing for a much larger volume of the liver to be assessed. This capability, in contrast to the spot measurement of TE, probably accounts for the superior diagnostic performance of MRE in comparison with TE, especially for detection and staging of mild fibrosis that has been documented in the literature [22–36].

Technical approach for MRE

The basic approach for MRE consists of three steps (Fig. 2): 1. Generating shear waves in tissue, 2. Visualizing the propagating waves using a phase contrast sequence (MRE sequence), and 3. Processing the wave images to produce quantitative cross-sectional images depicting tissue stiffness.

Mechanical vibrations are applied to the abdomen at typical frequencies in the range of 40–200 Hz. A number of devices for generating shear waves have been described, including pneumatic, electromechanical, and piezoelectric systems [25, 37–39]. For brevity, this review

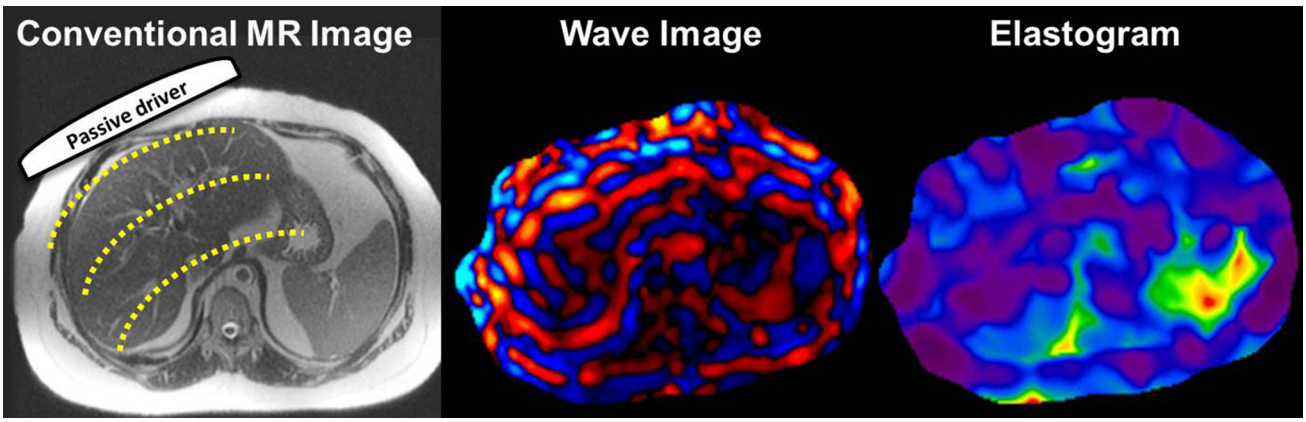

Fig. 2. Basic principles of magnetic resonance elastography illustrated here with an example of liver MRE. A passive driver is placed over the right lobe of the liver which transmits the acoustic vibrations from active driver into the abdomen schematically shown on the conventional MR image. These vibrations generate mechanical shear waves (*yellow dotted lines*). Wave image obtained from a 2D-GRE-MRE sequence with motion encoding gradients synchronized with the active mechanical driver and gives a snapshot of the propagating shear waves. From the wave information, an automatic inversion algorithm produces a stiffness map also referred to as elastogram

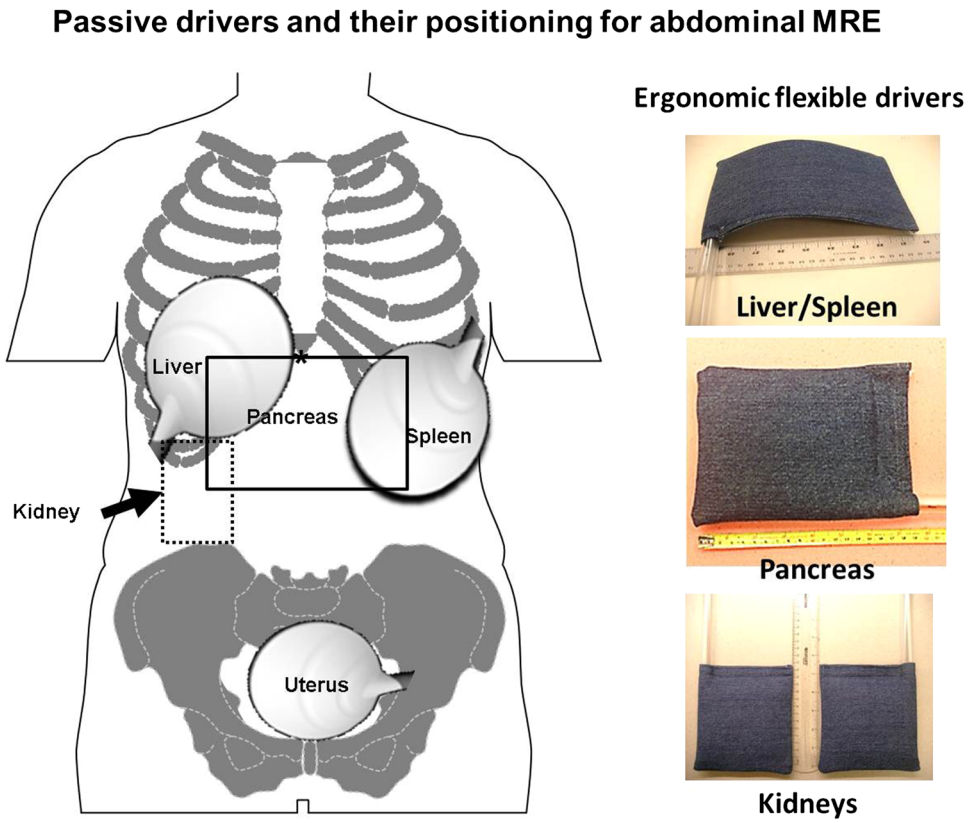

Fig. 3. Diagram showing placement of the passive drivers for MRE of the liver, pancreas, spleen, kidney, and uterus. Note for MRE of the liver, the driver is placed at the level of xiphisternum (*) and the driver for the kidney is placed on the back. Ergonomic flexible drivers that can be used for MRE of the liver/spleen, pancreas and the kidneys are shown (*inset*).

focuses on the standardized pneumatic driver system that is used in current FDA-approved commercial implementations of MRE. This system uses an acoustic wave generator that is placed outside the scanner room. A disk-shaped, nonmetallic drum-like "passive driver" is applied against the body wall and activated with acoustic pressure waves conducted via a 25-foot-long, flexible plastic tube connected to the wave generator to deliver shear waves to the tissues. .The passive driver can be easily applied against the body (Fig. 3) and placed under surface coil arrays commonly used for abdominal imaging. Newer flexible passive driver designs have improved ergonomics and may be useful for kidney and pancreas imaging [40, 41].

The MRE acquisition is a modified phase-contrast sequence [14, 42]. MRE sequences can be based on gradient-recalled echo (GRE), spin-echo (SE), balanced steady-state free precision, or echo-planar imaging (EPI) techniques. Special motion encoding gradients (MEGs) are used to sensitize the sequence to cyclic tissue motion caused by the shear waves. These gradients oscillate at the same frequency as the acoustic vibration that allows capturing the cyclic motion caused by shear waves with amplitudes as small as fractions of microns [42–44]. The timing relationship between the applied mechanical waves and the MEGs is varied to allow for snapshots of the waves in the tissue to be acquired during typically three or four phases of the wave cycle. Immediately after the wave images are acquired, the MRI system typically processes them to calculate corresponding elastograms. The wave images undergo several pre-processing steps including phase unwrapping, directional filtering, and removal of gradient field effects before inversion [3]. In research studies, many kinds of processing algorithms have been evaluated including local spatial frequency, phase gradient, direct inversion of the wave equation, and finite-element-based iterative methods [3, 45–48].

The stiffness maps depict tissue stiffness across the cross section studied. Regions of interest (ROIs) can be drawn manually or using an automated segmentation algorithm to obtain shear stiffness of the organs.

MRE of liver

The most common clinical application of MRE in the abdomen is in the evaluation of chronic liver diseases. Multiple studies have demonstrated that MRE surpasses other noninvasive tests such as serum tests for liver

function [23, 24, 27] and TE [28] for detection and staging of liver fibrosis. Liver stiffness measured with MRE is not affected by the presence of liver fat alone [25]. MRE is easily performed in patients of different sizes [25, 49, 50]. MRE has high repeatability, reproducibility, and interobserver correlation for liver stiffness [22, 33, 34, 51].

Most clinical studies on MRE of the liver are performed after 4–6 h of fasting similar to a clinical liver MRI study. Follow-up studies would ideally be performed with similar conditions to ensure comparability as post-prandial status is known to cause increased liver stiffness in patients with liver fibrosis [52, 53]. Fasting is the best way to ensure repeatability of the liver stiffness measurements. The MRE sequence can be performed in any order during a liver MRI study, and administration of intravenous gadolinium contrast agents does not significantly influence the liver stiffness evaluation [54, 55]

The most widely used MRE technique is described here (Fig. 4). The pneumatic passive driver is placed in the right lower chest /upper abdomen in the mid clavicular line at the level of the xiphisternum so that the largest portion of the liver is directly under the driver [50]. The 2D-GRE MRE sequence is performed at 60 Hz, and four slices of 10-mm thickness are prescribed over the region of liver with the largest cross section. This is usually near the dome of the liver, but the dome should be avoided as there may be breath hold artifacts. The slices are obtained in expiration to ensure reproducibility of the position of the liver. Typical sequence parameters are as follows: repetition time/echo time (TR/TE) = 50/18.4 to 26 ms; matrix = 256 × 64; band width = 33 kHz; flip angle of 30, four phase offsets, and NEX = 1. The prescribed time to echo is dependent on the sequence installed, gradient performance, and adjusting other parameters. A time to echo of 18.4 ms is in the In-phase, and therefore beneficial in patients with fatty livers when the signal from the liver parenchyma would be the highest possible. Reducing the time to echo below 20 ms may also be useful in patients with iron overload as it would marginally increase signal from the liver. Breath hold duration is about 16–20 s depending on the size of the patient and field of view prescribed. Using parallel imaging with an acceleration factor of 2, each section can be acquired in duration of as short as 12 s.

Stiffness maps are automatically generated within a few minutes of completion of the MRE sequence (Fig. 5). Manufacturers have standardized the color scale of the stiffness maps and have adopted a default scale of 0–8 kPa for liver MRE. Liver stiffness can be quantified by drawing the ROI on the gray-scale stiffness maps taking care to avoid large vessels, liver edge, fissures, and gall bladder fossa that can be visualized on the magnitude images of the MRE sequence. Regions of wave interference that can be seen on wave images are also excluded for reliable stiffness estimation. A large geographic ROI provides an assessment of a larger volume

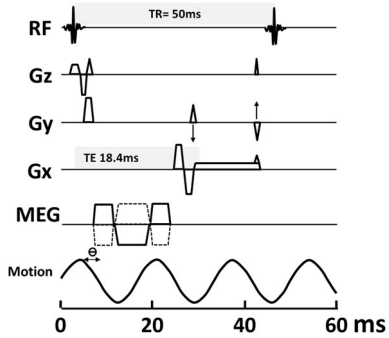

Fig. 4. Schematic diagram of a 2D GRE MRE pulse sequence. The TR (time to repeat) and TE (time to echo) in this illustration are 50 and 18.4 ms, respectively. Motion encoding gradients (MEGs) are synchronized with the applied vibration throughout image acquisition. The MEGs can be applied to sensitize the sequence to cyclic tissue motion in any of the *x*, *y*, or *z* directions, as shown. The phase relationship (Θ) between the MEGs and the acoustic waves can be adjusted in steps to acquire wave images at different phases of the cyclic motion. Note that TE is variable, and illustrated here is a TE of 18.4 so that signal is in the in-phase and gives maximum signal from the liver.

of liver than a few small elliptical ROIs. Larger ROIs can also be drawn using an automated segmentation algorithm [56]. The average stiffness from several slices is reported as the mean stiffness value in kilopascals (kPa). Liver stiffness with MRE is reproducible with >95% interobserver agreement [24, 34, 57] and has better agreement than that between pathologists staging liver fibrosis [58].

Normal liver stiffness is usually less than 2.5 kPa [22] and most studies have reported normal liver stiffness within a range of 1.54–2.87 kPa [49]. The influences of age, sex, race, and ethnicity on the measured normal liver parenchyma stiffness are not clearly understood; however, studies have not shown any significant association. Body mass index (BMI) as a single parameter is also not significantly associated with liver stiffness, and this is an advantage over TE which often does not give reliable results in patients with high BMI that are associated with a high failure rate [21, 22, 25, 33].

Detection and staging of liver fibrosis

MRE is the most promising noninvasive technique to replace or reduce the need for invasive liver biopsy, the current gold standard for detection and staging of liver fibrosis. Estimation of fibrosis content or burden is considered to be a better indicator of mild fibrosis than histologic staging of fibrosis [59, 60]. MRE correlates well with the fibrosis content of the liver and therefore may serve as an indicator for fibrosis burden [61]. Liver stiffness increases with increasing stage of fibrosis (Fig. 6).

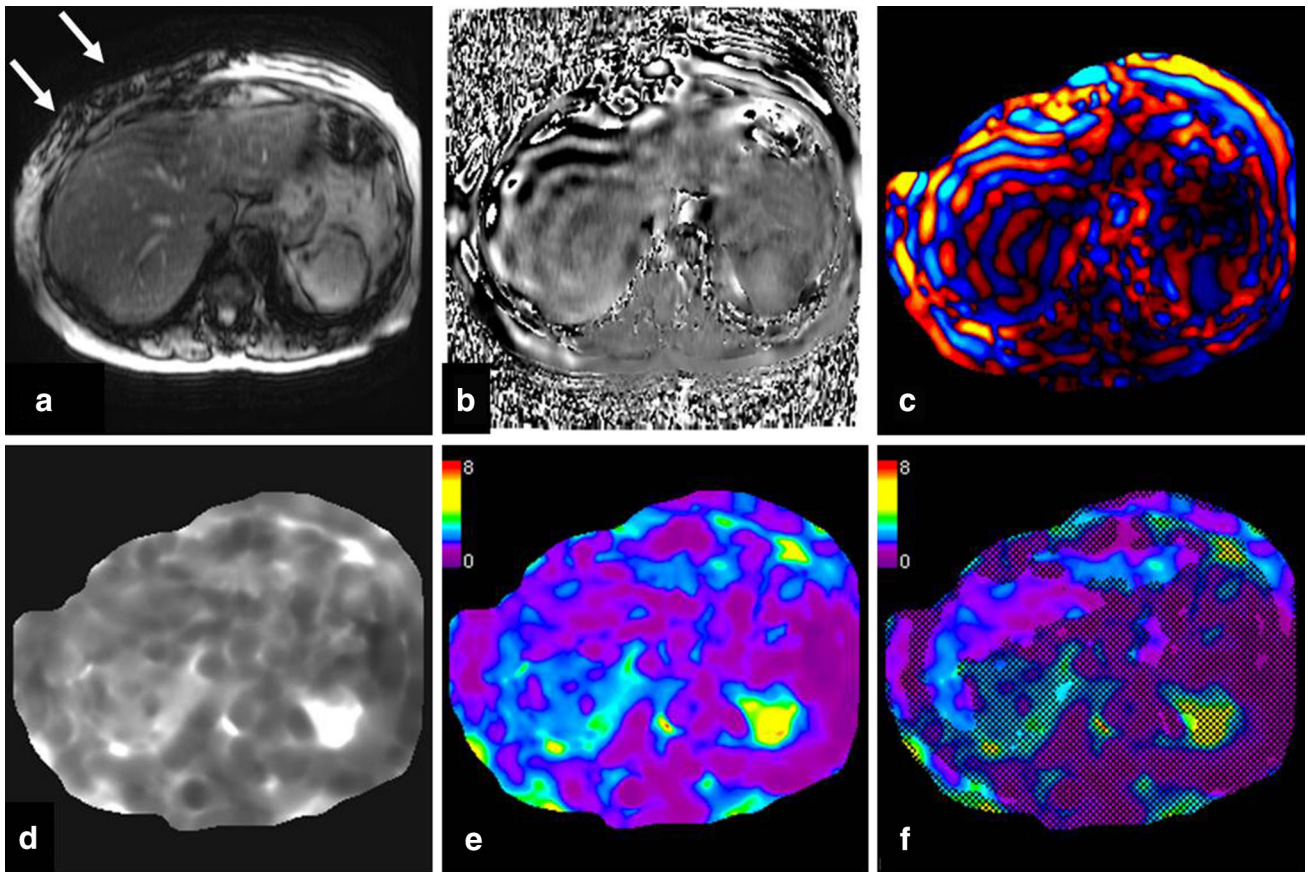

Fig. 5. An example of 2D-GRE-MRE sequence of the liver with raw data and processed images from inversion algorithm. Images from a single MRE slice through the liver produces raw magnitude (**A**) and (**B**) phase images. Note the signal loss due to intravoxel phase dispersion induced by acoustic waves (*white arrow*) produced by the driver opposed to the abdominal wall. Wave image (**C**) in *color* showing traversing shear waves through the cross section of the abdomen. *Gray scale* stiffness map (**D**) on which regions of interest can be drawn to measure tissue stiffness. *Color stiffness map* with *color scale* of 0–8 kPa (**E**) useful for a qualitative assessment. Confidence map (**F**) showing areas with less reliable stiffness (<95%) crossed out. Regions of interest should be drawn within the region not crossed out for valid stiffness measurement.

Multiple published studies have concluded that MRE has a high diagnostic performance in detection and staging of liver fibrosis. MRE can differentiate normal livers from fibrotic livers with an accuracy of ≥90% using a cut off stiffness values >2.4 kPa [23–25, 27]. MRE can also detect liver fibrosis when anatomical features of fibrosis and cirrhosis are absent [62]. The accuracy of MRE for detecting clinically significant fibrosis and cirrhosis are >95% and 98%, respectively [23–25, 27, 28, 35, 36]. The high performance of MRE has been demonstrated in chronic liver diseases of different etiologies by several investigators.

MRE has a high positive predictive value for ruling in significant fibrosis and a high negative predictive value for ruling out cirrhosis which is very useful for clinical decisions in the management of chronic liver diseases [49]. It should, however, be noted that liver stiffness may be increased with severe acute inflammation of the liver (acute hepatitis), acute flare of chronic hepatitis, portal hypertension, passive congestion due to cardiac failure, and acute biliary obstruction [63]. MRE of the liver for assessment of liver fibrosis is best avoided when these conditions are known to coexist. However, MRE may be performed when confounding factors such as acute inflammation or acute biliary obstruction have resolved.

Chronic liver diseases like viral hepatitis, autoimmune hepatitis, and steatohepatitis are characterized by liver fibrosis and inflammation, and some studies have shown that the presence of hepatitis activity may influence liver stiffness measured with MRE [64, 65], whereas another study did not show any such influence [24]. The effect of necroinflammation leading to overestimation of liver stiffness is most significant in livers with a mild degree of fibrosis (≤stage 2), leading to misclassification of fibrosis in lower stages [24]. Liver stiffness should therefore be interpreted carefully when serum alanine amino transferase levels are high indicating the presence of inflammation when mild fibrosis is suspected. Rarely a liver biopsy may be needed to confirm when the clinical suspicion of fibrosis is high and MRE results are not concordant.

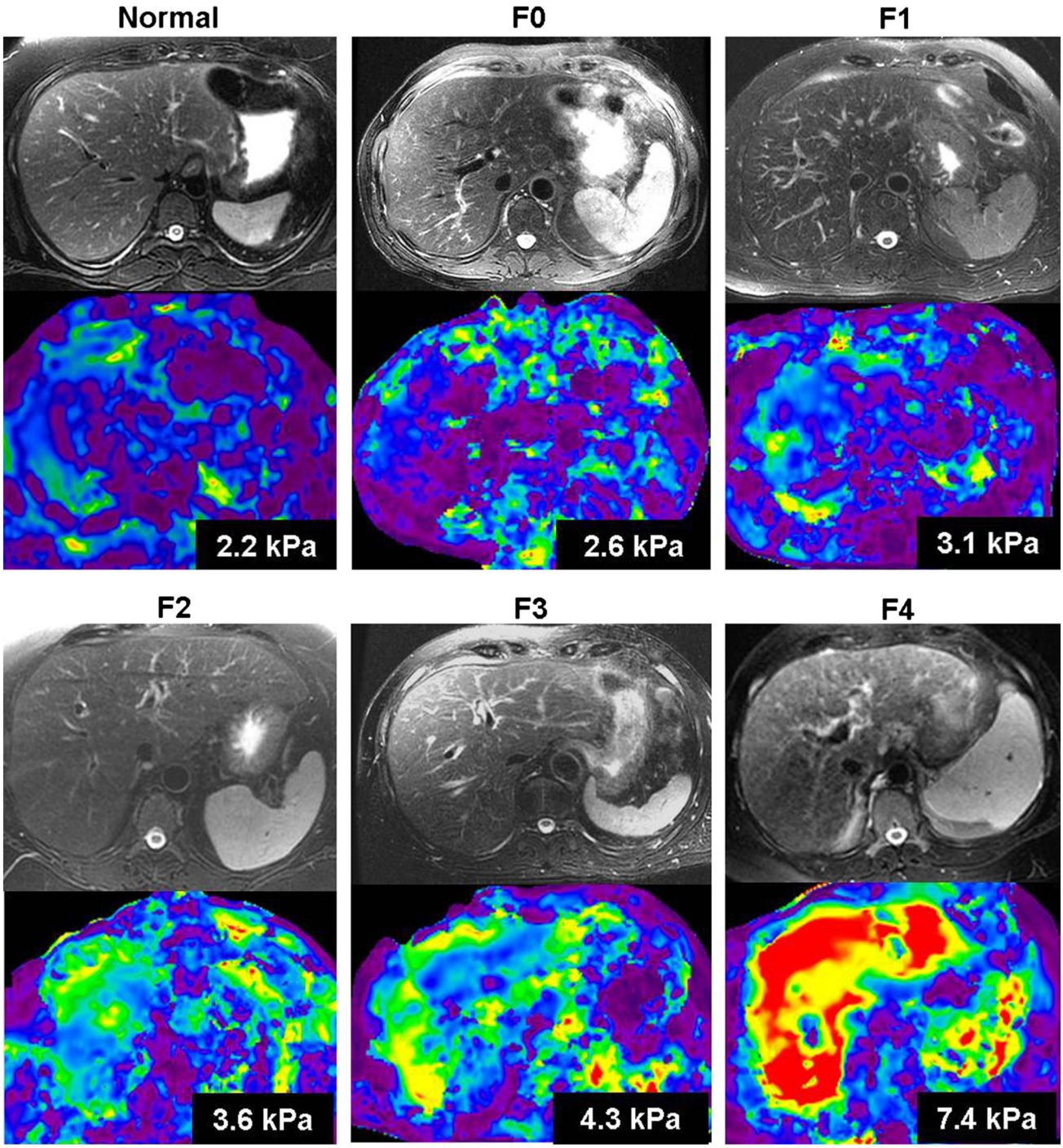

Fig. 6. Liver stiffness increases with increasing fibrosis stage. Axial fat suppressed T2-weighted images and stiffness maps from a normal healthy volunteer and five different chronic hepatitis C patients with biopsy confirmed fibrosis (METAVIR stages F0 through F4). The numbers on stiffness maps are mean liver stiffness.

MRE in non-alcoholic fatty liver disease (NAFLD)

NAFLD is the most common cause of chronic liver disease in adults in the United States and is increasing in prevalence among children and adolescents [66–68]. NAFLD has a spectrum consisting of simple steatosis, steatohepatitis (NASH) with or without fibrosis, and finally progression to cirrhosis and development of complications including hepatocellular carcinoma. Patients with NASH and those with advanced fibrosis are at particularly high risk of adverse outcomes and require more intense monitoring and therapy. As mentioned earlier, the presence of fat alone does not affect the evaluation of fibrosis in the liver. Simple steatosis in

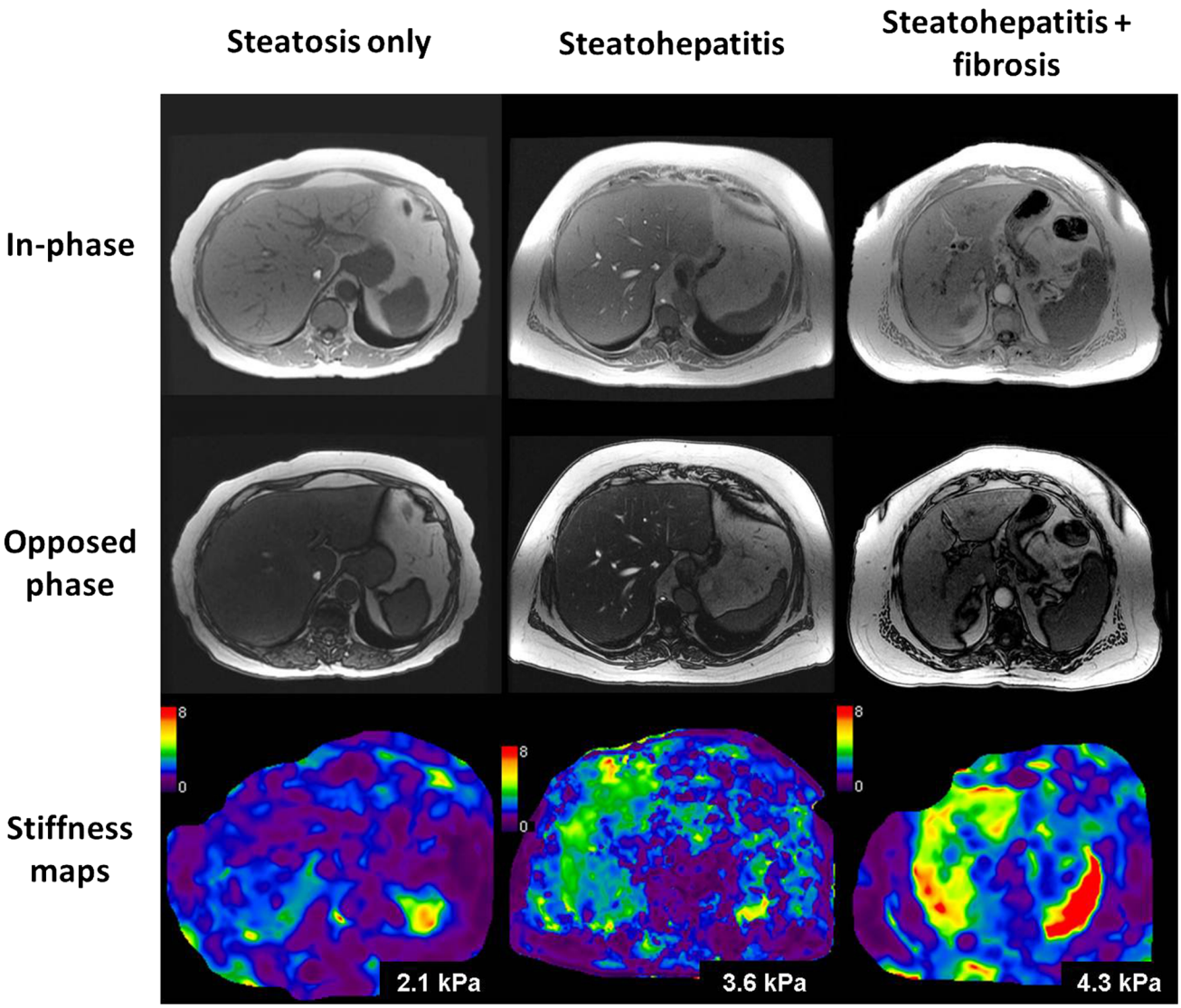

Fig. 7. Utility of MRE in the evaluation of non-alcoholic fatty liver disease (NAFLD). Examples of patients with biopsy-proven simple steatosis (*first column*), non-alcoholic steatohepatitis (*second column*), and steatohepatitis with fibrosis (*third column*). In-phase (*top row*), opposed-phase (*middle row*) images from fast gradient sequence and stiffness maps (*bottom row*). The mean liver stiffness values were 2.1, 3.6, and 4.3 kPa, respectively.

isolation does not cause any increased liver stiffness; however, NASH with or without fibrosis can cause increased stiffness that is readily detectable with MRE (Fig. 7) [69]. MRE can differentiate steatohepatitis from normal liver with an accuracy of 93% [69], and advanced fibrosis (stage 3-4) from stage 0-2 fibrosis with an accuracy range of 0.92 to 0.95 [70, 71]. MRE can therefore be useful for noninvasive diagnosis of advanced fibrosis in NAFLD. With MRE and MR fat quantification techniques, MRI can serve as a one-stop technique in the evaluation of NAFLD [72].

Portal hypertension and varices

Portal hypertension due to chronic liver disease results from liver fibrosis and associated architectural distortion and changes in the vasculature. Increased liver stiffness is associated with esophageal varices and is useful to predict esophageal varices [73–75]. MRE may be more accurate than TE for prediction of varices. In one study, MRE had an accuracy of 0.86 for the presence of esophageal varices and 0.81 for varices with a high bleeding risk [75], but in another study, there was no association between liver stiffness and presence of esophageal varices [76]. However, in a recent study with 3D MRE [77], both hepatic stiffness and splenic stiffness were associated with esophageal varices, and the performance of MRE was comparable with dynamic contrast-enhanced imaging for predicting the presence of esophageal varices and high-risk varices. Combined assessment of contrast-enhanced imaging and MRE

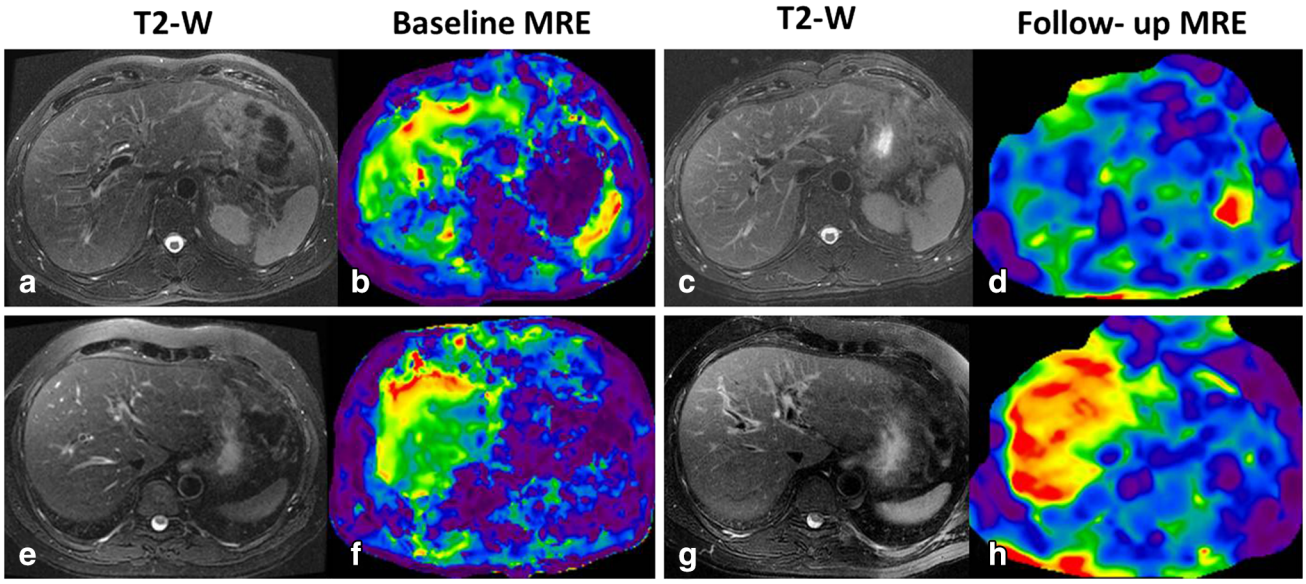

Fig. 8. Utility of liver MRE in longitudinal clinical follow-up. *Top row* (**A**–**D**) A case of chronic hepatitis C with baseline liver stiffness of 4.2 kPa (**B**), and a follow-up MRE after 3 years following antiviral treatment showed reduced liver stiffness to 2.8 kPa suggestive of response to treatment. *Bottom row* (**E**–**H**) Another case of chronic hepatitis C with a baseline liver stiffness of 4.2 kPa who showed progression of disease with liver stiffness increasing to 6.3 kPa within one year. This patient later developed portal hypertension on follow-up with stiffness increasing to 9.2 kPa after 3 years (not shown). Note there are no significant morphological changes in liver on the T2-weighted images for both cases.

significantly increased the detection of varices of any grade compared with dynamic contrast-enhanced imaging alone (85% vs. 74%) suggesting added value of MRE in patients with portal hypertension.

Compensated and decompensated liver cirrhosis

Patients with cirrhosis are further classified into compensated and decompensated cirrhosis based on the presence of variceal bleeding, ascites, or hepatic encephalopathy. The outcome in decompensated liver cirrhosis is worse than in those with compensated liver cirrhosis [78]. In a meta-analysis study, Singh et al. showed that liver stiffness measured with MRE is associated with the increased risk of decompensation, development of hepatocellular carcinoma, and death [79].

In another study [80], MRE was independently associated with decompensation. In patients with compensated cirrhosis, the hazard for hepatic decompensation was 1.42 (95% CI 1.16–1.75) per unit increase in liver shear stiffness over time. The hazard of hepatic decompensation was 4.96 (95% CI 1.4–17.0, $p = 0.019$) for a subject with compensated disease, and mean liver stiffness value was ≥5.8 kPa compared with an individual with compensated disease and lower mean liver stiffness values. These studies provide evidence for the role of MRE of the liver in prognostication and prediction of clinical outcomes in advanced fibrosis or cirrhosis.

Other applications of MRE in liver

MRE of the liver may be useful in the follow-up of chronic liver disease. Histologic staging of liver fibrosis is not sensitive enough to detect minor changes in liver fibrosis amount or fibrosis progression, and change in histologic stage does not always reflect change in fibrosis burden as it involves subjective interpretation of anatomical changes and not an objective assessment of amount of fibrosis. Histology is therefore not suitable for monitoring therapies that are designed to stop or cause regression of fibrosis [81]. As MRE-measured liver stiffness correlates with fibrosis content [61], it may be useful in demonstrating progression or improvement of liver stiffness during clinical follow-up (Fig. 8).

MRE may be useful in the evaluation of focal liver lesions. Preliminary studies have indicated that malignant liver tumors have higher stiffness than benign tumors and normal liver [82, 83]. Future studies are awaited for confirmation of results from the preliminary studies and for possible clinical application in characterization of focal liver lesions.

MRE of liver transplants can also be performed and has been found useful in the detection of advanced fibrosis in the liver transplants with recurrence of chronic liver disease [31, 84, 85]. MRE is also useful in the evaluation of congestive livers in post Fontan surgery patients for detection of liver fibrosis [86, 87]. Passively congested livers may be stiff without any fibrotic changes, and therefore further studies of these patients with

MRE are required to establish the correlation between congestion and liver stiffness.

Limitations of liver MRE

2D GRE-MRE is sensitive to the presence of iron in the liver, and therefore MRE may technically fail in patients with high liver iron content. The presence of iron results in poor signal from the liver, but is not known to affect stiffness properties. The shear waves still travel through the liver, but the signal from the liver is poor for a valid MRE. Newer sequences with low echo times that can improve liver signal have been developed and are useful in these livers [88]. Similar to other body MRI sequences, MRE may be limited in patients who are poor and inconsistent breath holders. Patients can be coached for breath holding for increased cooperation. One may also modify the MRE sequence, for example, decreasing FOV as much as possible or reducing the matrix size (at the cost of resolution) to reduce the breath hold time and obtain a valid result.

MRE of spleen

Splenomegaly is a common finding in patients with cirrhosis and non-cirrhotic portal hypertension and is probably due to increased portal venous pressure leading to congestion of blood in the spleen.

MRE of the spleen is best performed by placing the passive driver over the spleen, although propagation of the shear waves through the spleen can also be seen when MRE of the liver is performed [76, 89]. MRE performed with the passive driver over the spleen would ensure good propagation of shear waves through it resulting in reliable stiffness map generation. In general, MRE of the spleen is also performed at the same acoustic frequency of 60 Hz similar to liver. In earlier studies, splenic stiffness was found to correlate with splenic size, platelet count, and the presence of esophageal varices in patients with chronic liver disease [76, 90]. Spleen stiffness correlates with liver stiffness and, in patients with liver fibrosis, spleen stiffness increases in parallel with increasing liver stiffness [76]. A splenic stiffness greater than 10.5 kPa is predictive of esophageal varices (Fig. 9), suggesting the usefulness of splenic stiffness evaluation as a noninvasive method to assess portal hypertension. A large meta-analysis of studies on splenic stiffness measurement with ultrasound-based elastography techniques showed 78% sensitivity and 76% specificity for detection of any degree of esophageal varices based on pooled estimates, which is not accurate enough to support its use in routine clinical practice. There have been a limited number of large studies with MRE of the spleen; therefore, the role of MRE of spleen for noninvasive prediction of esophageal varices is difficult to ascertain. Recently, Shin et al. [38] using a 3D echo planar MRE technique demonstrated that both hepatic and splenic stiffness had positive linear correlations with the endoscopic grade of esophageal varices. In another study, spleen stiffness was found to have a significant correlation with the direct hepatic venous pressure gradient ($r^2 = 0.86$, $p < 0.001$) [91]. Another study by Ronot et al. [92] showed that spleen loss modulus was the best parameter for identifying patients with severe portal hypertension ($p = 0.019$, AUROC = 0.81) or high-risk varices ($p = 0.042$, AUROC = 0.93). Both studies suggest a promising role for MRE of the spleen in the evaluation of portal hypertension and significant esophageal varices

MRE of pancreas

Chronic pancreatitis results in fibrosis of the gland, and adenocarcinoma of the pancreas is associated with a scirrhous tissue reaction. These processes may increase the stiffness of the pancreas and hence the increased interest in exploring the technique of MRE for evaluation of the pancreas and its disorders.

The midline retroperitoneal location and small size of the pancreas poses a challenge to performing an MRE of this gland; however, an initial study showed the feasibility of this technique [93]. Recently Shi et al. [41] performed MRE in normal volunteers using a modified ergonomic flexible driver. As the gland is small, several modifications were needed to ensure a valid stiffness estimation. A three-dimensional (3D) spin-echo echo planar imaging (SE-EPI) MRE sequence operating at 40 Hz was found to be the most suitable (Fig. 10). A direct inversion algorithm was also used to estimate tissue stiffness. As the pancreas is related to the stomach above, subjects for MRE should have an empty stomach so that the distance between the driver on the skin and the pancreas is reduced to ensure good wave propagation. This also would minimize any compression of the pancreas by a full stomach. The mean stiffness of a normal pancreas at 40 Hz was 1.15 ± 0.17 kPa, and at 60 Hz, the stiffness was similar to a normal liver parenchyma.

The initial studies have shown the feasibility of performing MRE of the pancreas and results from studies evaluating its role in chronic pancreatitis and pancreatic cancers (Fig. 11) are eagerly awaited.

MRE of kidneys

The retroperitoneal location of the kidneys poses challenges for the propagation of shear waves through them. In a preliminary study, the feasibility of MRE of the kidneys in healthy volunteers with subjects lying supine on an external driver was demonstrated [94]. It is also possible to design smaller drivers to be placed in contact with the back closer to the kidneys to ensure good propagation of shear waves, and this technique is still under evaluation. In view of the small size of the kidneys,

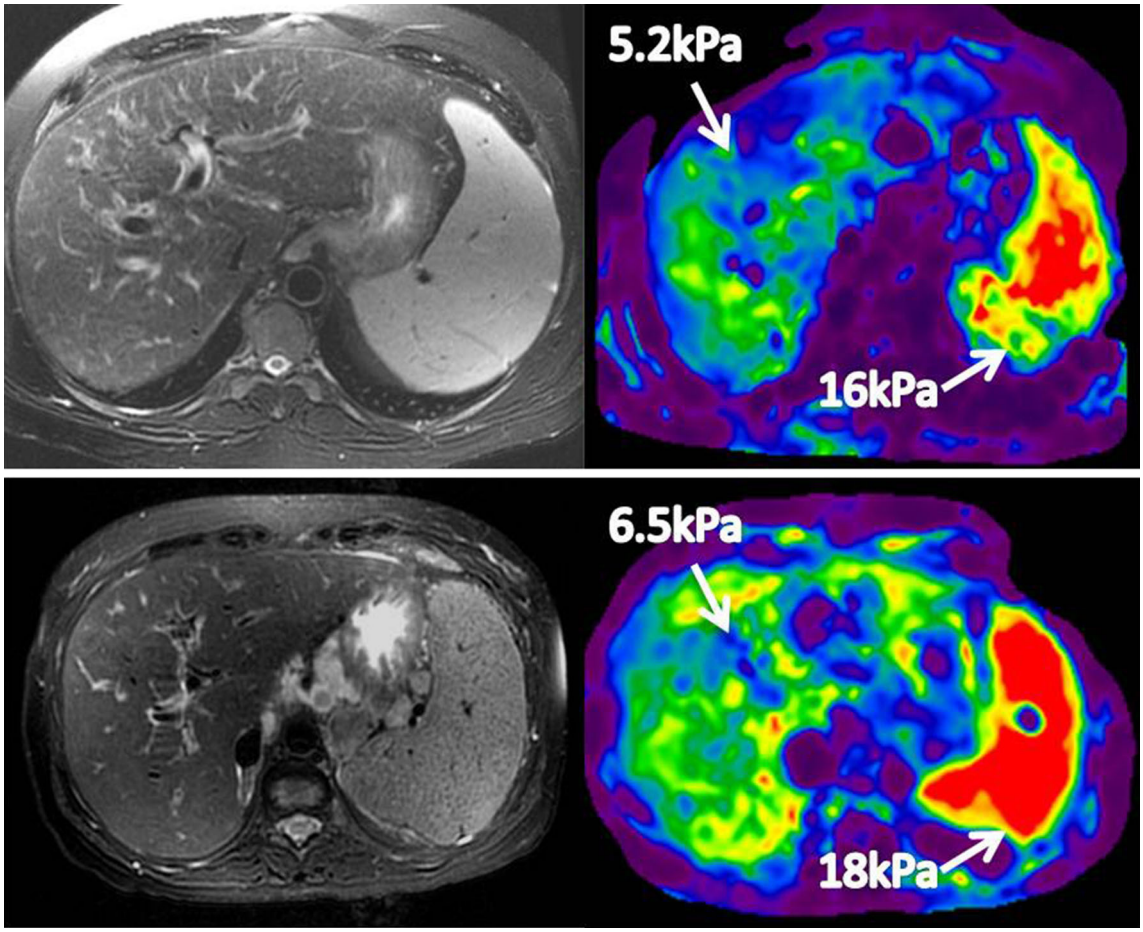

Fig. 9. MRE of the spleen. *Top row* A patient with chronic hepatitis C cirrhosis with portal gastropathy and esophageal varices. *Bottom row* Another patient with cryptogenic cirrhosis with portal hypertension, esophageal varices and ascites. In both cases, the splenic stiffness is more than 10 kPa.

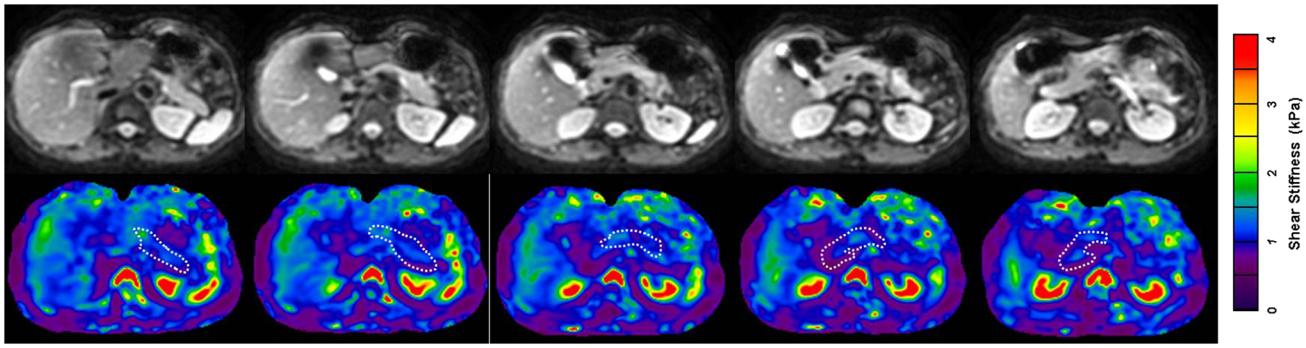

Fig. 10. MRE of normal pancreas with 3D-EPI MRE technique performed at 40 Hz. Magnitude images (*top row*) and stiffness maps (*bottom row*) showing tail, body, neck, head, and uncinate parts of the pancreas. Note the homogeneous appearance of the pancreas on the stiffness maps. (Image courtesy—Dr. Yu Shi, Radiology, Shengjing hospital, China Medical University, Shenyang, Liaoning, China).

a higher frequency (90 Hz,) and a 3D MRE technique similar to that described for MRE of the pancreas would be suitable. MRE studies of the kidneys can be obtained in various planes, but the coronal plane including both kidneys would be useful for comparison (Fig. 12).

Renal stiffness is dependent on its tissue components. Kidneys are perfused richly with ~25% of the cardiac output. Nearly one fourth of the renal volume under normal physiological status can be attributed to blood pressure, blood within the kidneys, the glomerular filtrate within the tubules,

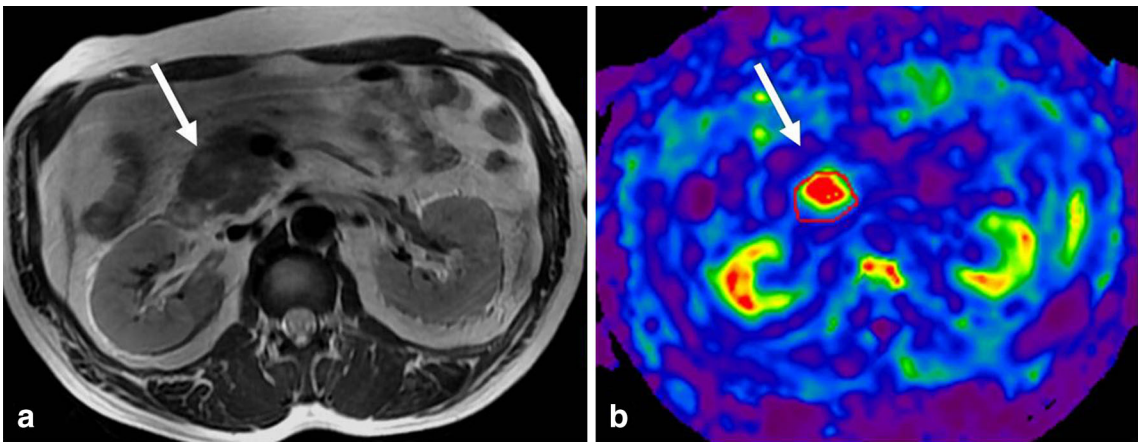

Fig. 11. MRE of pancreas performed at 40 Hz. Axial T2-weighted image (**A**) shows a mildly hyperintense mass in the head of pancreas representing histology-proven well-differentiated adenocarcinoma. Stiffness map (**B**) showing increased stiffness of the mass at 2.9 kPa, significantly higher than normal pancreas stiffness of 1.1 kPa (Image courtesy—Dr. Yu Shi, Radiology, Shengjing hospital, China Medical University, Shenyang, Liaoning, China).

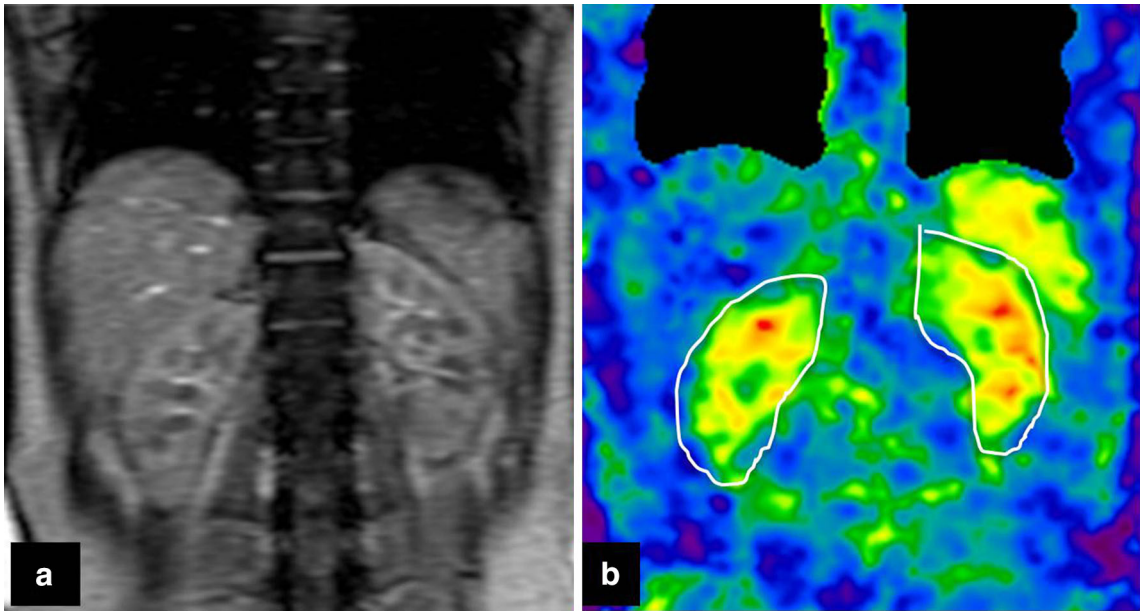

Fig. 12. MRE of the native kidneys performed at 90 Hz in coronal plane in a normal healthy volunteer. A single large driver was placed in midline with the volunteer lying supine over the driver. Stiffness map (**B**) demonstrating symmetric stiffness distribution in the kidneys (outlined). The mean stiffness of the kidneys was 6.4 kPa.

and urine [95]. Renal blood flow may contribute significantly to the measured stiffness of the kidneys [96]. Anisotropy of the renal tissue may also impact on the stiffness evaluated in the kidney [97, 98]. The medulla is predominantly composed of tubular structures like vasa recta, collecting tubules, and Henle loops that run from the capsule to the papilla making it highly anisotropic compared with the cortex made of predominantly glomeruli and proximal tubules. Urinary obstruction may also influence the stiffness as it may increase the intrarenal pressure. The contribution of above mentioned anatomical and physiological factors with measured renal stiffness need to be further studied for its clinical use.

In a study with young healthy adults at 45-Hz frequency, Rouviere et al. [99] showed that MRE of the kidney was reproducible with an intrasubject variability of only 6%. In a recent study, high-resolution MRE of the kidney was performed in nine healthy volunteers. In this study, the renal medulla was shown to have a higher stiffness than the cortex [100] which may be attributed to the complex tubular structure and more interstitium in the medulla. More definitive information on the regional variation of renal stiffness may be obtained with 3D MRE evaluation. Larger studies exploring the utility of MRE in chronic renal

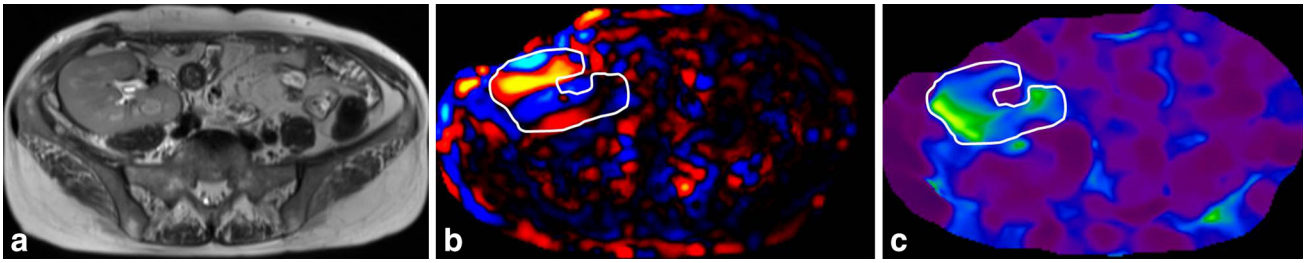

Fig. 13. MRE of a normal functioning transplant kidney performed at 90 Hz. Axial T2-weighted image (**A**) showing a normal size renal graft in the right iliac fossa. Wave image (**B**) demonstrating propagation of shear waves through the graft and a stiffness map (**C**) with graft outlined. The mean stiffness of the graft was 6.8 kPa.

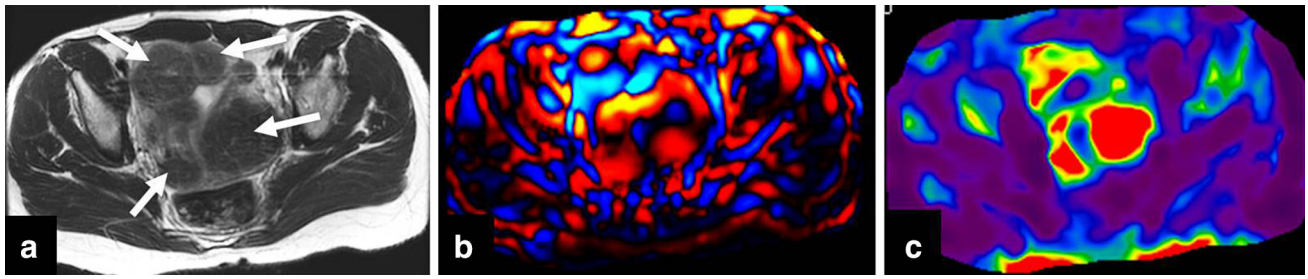

Fig. 14. MRE of a fibroid uterus performed at 60 Hz. Axial T2-weighted image (**A**) showing several hypointense fibroids (*arrows*), wave image (**B**) showing excellent propagation of the shear waves through the uterus and fibroids. Stiffness map (**C**) showing stiff areas corresponding to the fibroids.

parenchymal disease are currently not available and are eagerly awaited.

Few studies have focused on MRE of the renal transplant. MRE of the renal transplant is technically easier to perform as renal transplants are usually located in the iliac fossa and therefore subject to less respiratory movement. They also are near to skin surface which facilitates better propagation of shear waves and less attenuation of high-frequency shear waves (Fig. 13). In a preliminary study, a trend of increased stiffness in the transplants of patients with a mild or moderate degree of interstitial fibrosis was found with no significant differences [101]. In another preliminary study, higher stiffness was found in patients without interstitial fibrosis compared to those with fibrosis [102]. The preliminary studies show a complex relationship between renal stiffness, and the pathological processes in a renal transplant and needs to be further evaluated. MRE of renal transplants is another exciting area for future study and may be valuable in the evaluation of grafts in the future.

MRE of uterus

The mechanical integrity of the uterine cervix is important for a successful pregnancy. Altered tissue structure may result in significant changes in the mechanical properties of the cervix and result in premature delivery. A noninvasive method to assess stiffness of the uterus and cervix may be useful in understanding mechanical factors affecting premature delivery and infertility. Knowledge of mechanical properties of normal uterus and cervix may also be useful in differentiation of focal lesions arising from these organs.

3D MRE of the uterus in healthy female volunteers showed that the uterine corpus had a higher elasticity but similar viscosity compared with cervix [103]. In this study, it was also found that stiffness of both endometrium and myometrium decreased during the menstrual cycle. More studies are required to confirm these preliminary findings.

Uterine fibroids or leiomyoma are common and frequently associated with pelvic symptoms and infertility. Fibroids have variable composition, and evaluation of the stiffness of the fibroids may give insights into their composition for treatment planning such as hi-frequency ultrasound (HiFU). Mechanotransduction is thought to be a significant factor affecting the growth of uterine fibroids. Stiffness of fibroids may contribute to their growth [104] and possibly their recurrence.

In a preliminary study, Stewart et al. [105] performed MRE of the uterus in a supine position with the passive driver placed on the lower abdomen overlying the uterus. A 2D-GRE MRE sequence at 60 Hz acoustic frequency similar to that of liver MRE was used (Fig. 14). They demonstrated variable stiffness of the fibroids that probably represents different composition of the fibroids.

However, this was not histologically correlated, and future studies in this direction are required. The fibroids studied had an average stiffness of 5.09 kPa (range 3.95–6.68 kPa). The size of the fibroids studied was in the range of 4.5–22.5 cm. Evaluation of tiny fibroids may be best done with a 3D MRE sequence. In another study, Hesley et al. [106] showed that fibroids became stiffer after HiFU. Results from these preliminary studies are encouraging and provide motivation for future studies on stiffness of uterine fibroids and its correlation with histological findings for characterization of the fibroids. Assessment of mechanical properties of uterine fibroids may be useful for prediction of their growth and predicting treatment outcomes.

MRE of other abdominal organs

Successful clinical application of MRE of the liver and its increasing utility have stirred interest in evaluation of other abdominal organs. Evaluation of prostate via transrectal and transperineal approaches has been described [107, 108]. Other organs to be explored include bowel and urinary bladder. These organs are technically challenging owing to their location, mobility, physiological motion, and/or small size of tissue (wall thickness) to be studied. However, newer innovations in MRE may soon make it possible to evaluate these organs.

Conflict of interest No conflicts of interest to declare.

References

1. Fung YC, Liu SQ (1993) Elementary mechanics of the endothelium of blood vessels. J Biomech Eng 115:1–12
2. Gierke HE, Oestreicher HL, Franke EK, Parrack HO, WIttern WW (1952) Physics of vibrations in living tissues. J Appl Physiol 4:886–900
3. Manduca A, Oliphant T, Dresner M, et al. (2001) Magnetic resonance elastography: non-invasive mapping of tissue elasticity. Med Image Anal 5:237–254
4. Oliphant TE, Manduca A, Ehman RL, Greenleaf JF (2001) Complex-valued stiffness reconstruction for magnetic resonance elastography by algebraic inversion of the differential equation. Magn Reson Med 45:299–310
5. Sarvazyan AP (1982) Acoustic properties of tissues relevant to therapeutic applications. Br J Cancer Suppl 5:52–54
6. Sarvazyan AP, Skovoroda AR, Emelianov SY, et al. (1995) Biophysical bases of elasticity imaging. In: Jones JP (ed) *Acoustic imaging*. New York: Plenum, pp 223–240
7. Sarvazyan AP, Rudenko OV, Swanson SD, Fowlkes JB, Emelianov SY (1998) Shear wave elasticity imaging: a new ultrasonic technology of medical diagnostics. Ultrasound Med Biol 24:1419–1435
8. Sarvazyan A, Hall TJ, Urban MW, et al. (2011) An overview of elastography: an emerging branch of medical imaging. Curr Med Imaging Rev 7:255–282
9. Sarvazyan AP, Urban MW, Greenleaf JF (2013) Acoustic waves in medical imaging and diagnostics. Ultrasound Med Biol 39:1133–1146
10. Wilson LS, Robinson DE, Dadd MJ (2000) Elastography—the movement begins. Phys Med Biol 45:1409–1421
11. Gao L, Parker KJ, Lerner RM, Levinson SF (1996) Imaging of the elastic properties of tissue—a review. Ultrasound Med Biol 22:959–977
12. Greenleaf JF, Muthupillai R, Rossman PJ, et al. (1997) Measurement of tissue elasticity using magnetic resonance elastography. Rev Prog Quant Nondestr Eval 16:19–26
13. Greenleaf JF, Fatemi M, Insana M (2003) Selected methods for imaging elastic properties of biological tissues. Annu Rev Biomed Eng 5:57–78
14. Muthupillai R, Lomas D, Rossman P, et al. (1995) Magnetic resonance elastography by direct visualization of propagating acoustic strain waves. Science 269:1854–1857
15. Mariappan YK, Glaser KJ, Ehman RL (2010) Magnetic resonance elastography: a review. Clin Anat 23:497–511
16. Glaser KJ, Manduca A, Ehman RL (2012) Review of MR elastography applications and recent developments. J Magn Reson Imaging 36:757
17. Sandrin L, Fourquet B, Hasquenoph JM, et al. (2003) Transient elastography: a new noninvasive method for assessment of hepatic fibrosis. Ultrasound Med Biol 29:1705–1713
18. de Ledinghen V, Douvin C, Kettaneh A, et al. (2006) Diagnosis of hepatic fibrosis and cirrhosis by transient elastography in HIV/hepatitis C virus-coinfected patients. J Acquir Immune Defic Syndr 41:175–179
19. Talwalkar J, Kurtz D, Schoenleber S, West C, Montori V (2007) Ultrasound-based transient elastography for the detection of hepatic fibrosis: systematic review and meta-analysis. Clin Gastroenterol Hepatol 5:1214–1220
20. Friedrich-Rust M, Ong MF, Martens S, et al. (2008) Performance of transient elastography for the staging of liver fibrosis: a meta-analysis. Gastroenterology 134:960–974
21. Castera L (2011) Invasive and non-invasive methods for the assessment of fibrosis and disease progression in chronic liver disease. Best Pract Res Clin Gastroenterol 25:291–303
22. Venkatesh SK, Wang G, Teo LL, Ang BW (2014) Magnetic resonance elastography of liver in healthy Asians: normal liver stiffness quantification and reproducibility assessment. J Magn Reson Imaging 39(1):1–8
23. Ichikawa S, Motosugi U, Ichikawa T, et al. (2012) Magnetic resonance elastography for staging liver fibrosis in chronic hepatitis C. Magn Reson Med Sci 11:291–297
24. Venkatesh SK, Wang G, Lim SG, Wee A (2014) Magnetic resonance elastography for the detection and staging of liver fibrosis in chronic hepatitis B. Eur Radiol 24:70–78
25. Yin M, Talwalkar J, Glaser K, et al. (2007) Assessment of hepatic fibrosis with magnetic resonance elastography. Clin Gastroenterol Hepatol 5(1207–1213):e1202
26. Huwart L, Peeters F, Sinkus R, et al. (2006) Liver fibrosis: noninvasive assessment with MR elastography. NMR Biomed 19:173–179
27. Huwart L, Sempoux C, Salameh N, et al. (2007) Liver fibrosis: noninvasive assessment with MR elastography versus aspartate aminotransferase-to-platelet ratio index. Radiology 245:458–466
28. Huwart L, Sempoux C, Vicaut E, et al. (2008) Magnetic resonance elastography for the noninvasive staging of liver fibrosis. Gastroenterology 135:32–40
29. Huwart L, Salameh N, ter Beek LC, et al. (2008) MR elastography of liver fibrosis: preliminary results comparing spin-echo and echo-planar imaging. Eur Radiol 18:2535–2541
30. Kim BH, Lee JM, Lee YJ, et al. (2011) MR elastography for noninvasive assessment of hepatic fibrosis: experience from a tertiary center in Asia. J Magn Reson Imaging 34:1110–1116
31. Lee VS, Miller FH, Omary RA, et al. (2012) Magnetic resonance elastography and biomarkers to assess fibrosis from recurrent hepatitis C in liver transplant recipients. Transplantation 92:581–586
32. Lee DH, Lee JM, Han JK, Choi BI (2013) MR elastography of healthy liver parenchyma: Normal value and reliability of the liver stiffness value measurement. J Magn Reson Imaging 38(5):1215–1223
33. Lee YJ, Lee JM, Lee JE, et al. (2014) MR elastography for noninvasive assessment of hepatic fibrosis: Reproducibility of the examination and reproducibility and repeatability of the liver stiffness value measurement. J Magn Reson Imaging 39(2):326–331
34. Hines CDG, Bley TA, Lindstrom MJ, Reeder SB (2010) Repeatability of magnetic resonance elastography for quantification of hepatic stiffness. J Magn Reson Imaging 31:725–731
35. Asbach P, Klatt D, Schlosser B, et al. (2010) Viscoelasticity-based staging of hepatic fibrosis with multifrequency MR elastography. Radiology 257:80–86

36. Asbach P, Klatt D, Hamhaber U, et al. (2008) Assessment of liver viscoelasticity using multifrequency MR elastography. Magn Reson Med 60:373–379
37. Rouviere O, Yin M, Dresner MA, et al. (2006) MR elastography of the liver: preliminary results. Radiology 240:440–448
38. Huwart L, Peeters F, Sinkus R, et al. (2006) Liver fibrosis: non-invasive assessment with MR elastography. NMR Biomed 19:173–179
39. Klatt D, Asbach P, Rump J, et al. (2006) In vivo determination of hepatic stiffness using steady-state free precision magnetic resonance elastography. Investig Radiol 41:841–848
40. Chen J, Stanley D, Glaser K, Yin M, Rossman P, Ehman R (2010) Ergonomic flexible drivers for hepatic MR elastography. In: Annual meeting of international society for magnetic resonance in medicine, Stockholm, Sweden
41. Shi Y, Glaser KJ, Venkatesh SK, Ben-Abraham EI, Ehman RL (2014) Feasibility of using 3D MR elastography to determine pancreatic stiffness in healthy volunteers. J Magn Reson Imaging. doi:10.1002/jmri.24572
42. Muthupillai R, Lomas DJ, Rossman PJ, et al. (1996) Visualizing propagating transverse mechanical waves in tissue-like media using magnetic resonance imaging. Acoust Imaging 22:279–283
43. Rump J, Klatt D, Braun J, Warmuth C, Sack I (2007) Fractional encoding of harmonic motions in MR elastography. Magn Reson Med 57:388–395
44. Glaser KJ, Felmlee JP, Ehman RL (2006) Rapid MR elastography using selective excitation. Magn Reson Med 55:1381–1389
45. Manduca A, Dutt V, Borup DT, et al. (1998) An inverse approach to the calculation of elasticity maps for magnetic resonance elastography. Med Imaging 3338:426–436
46. Manduca A, Lake D, Kruse S, Ehman R (2003) Spatio-temporal directional filtering for improved inversion of MR elastography images. Med Image Anal 7:465–473
47. Chen Q, Ringleb SI, Manduca A, Ehman RL, An KN (2005) A finite element model for analyzing shear wave propagation observed in magnetic resonance elastography. J Biomech 38:2198–2203
48. Chen Q, Ringleb SI, Manduca A, Ehman RL, An KN (2006) Differential effects of pre-tension on shear wave propagation in elastic media with different boundary conditions as measured by magnetic resonance elastography and finite element modeling. J Biomech 39:1428–1434
49. Venkatesh SK, Yin M, Ehman RL (2013) Magnetic resonance elastography of liver: clinical applications. J Comput Assist Tomogr 37:887–896
50. Venkatesh SK, Yin M, Ehman RL (2013) Magnetic resonance elastography of liver: technique, analysis, and clinical applications. J Magn Reson Imaging 37:544–555
51. Godfrey EM, Patterson AJ, Priest AN, et al. (2012) A comparison of MR elastography and P-31 MR spectroscopy with histological staging of liver fibrosis. Eur Radiol 22:2790–2797
52. Yin M, Talwalkar JA, Glaser KJ, et al. (2011) Dynamic postprandial hepatic stiffness augmentation assessed with MR elastography in patients with chronic liver disease. AJR Am J Roentgenol 197:64–70
53. Hines CDG, Lindstrom MJ, Varma AK, Reeder SB (2011) Effects of postprandial state and mesenteric blood flow on the repeatability of MR elastography in asymptomatic subjects. J Magn Reson Imaging 33:239–244
54. Motosugi U, Ichikawa T, Sou H, et al. (2012) Effects of gadoxetic acid on liver elasticity measurement by using magnetic resonance elastography. Magn Reson Imaging 30:128–132
55. Hallinan JT, Alsaif HS, Wee A, Venkatesh SK (2014) Magnetic resonance elastography of liver: influence of intravenous gadolinium administration on measured liver stiffness. Abdom Imaging. doi:10.1007/s00261-014-0275-x
56. Dzyubak B, Glaser K, Yin M, et al. (2013) Automated liver stiffness measurements with magnetic resonance elastography. J Magn Reson Imaging 38:371–379
57. Motosugi U, Ichikawa T, Sano K, et al. (2010) Magnetic resonance elastography of the liver: preliminary results and estimation of inter-rater reliability. Jpn J Radiol 28:623–627
58. Runge JH, Bohte AE, Verheij J, et al. (2014) Comparison of interobserver agreement of magnetic resonance elastography with histopathological staging of liver fibrosis. Abdom Imaging 39(2):283–290
59. Caballero T, Pérez-Milena A, Masseroli M, et al. (2001) Liver fibrosis assessment with semiquantitative indexes and image analysis quantification in sustained-responder and non-responder interferon-treated patients with chronic hepatitis C. J Hepatol 34:740–747
60. Lazzarini AL, Levine RA, Ploutz-Snyder RJ, Sanderson SO (2005) Advances in digital quantification technique enhance discrimination between mild and advanced liver fibrosis in chronic hepatitis C. Liver Int 25:1142–1149
61. Venkatesh SK, Xu S, Tai D, Yu H, Wee A (2013) Correlation of MR elastography with morphometric quantification of liver fibrosis (Fibro-C-Index) in chronic hepatitis B. Magn Reson Med. doi:10.1002/mrm.25002
62. Venkatesh SK, Takahashi N, Glocker JF, et al. (2008) Non-invasive diagnosis of liver fibrosis: conventional MR imaging findings versus MR elastography. In: Proceedings of 17th annual meeting of ISMRM, Toronto, Canada (abstract 2613)
63. Venkatesh SK, Ehman RL (2014) Magnetic resonance elastography of liver. Magn Reson Imaging Clin N Am 22:433–446
64. Shi Y, Guo Q, Xia F, et al. (2014) MR elastography for the assessment of hepatic fibrosis in patients with chronic hepatitis B infection: does histologic necroinflammation influence the measurement of hepatic stiffness? Radiology 2014(273):88–98
65. Ichikawa S, Motosugi U, Nakazawa T, et al. (2014) Hepatitis activity should be considered a confounder of liver stiffness measured with MR elastography. J Magn Reson Imaging. doi:10.1002/jmri.24666
66. Younossi ZM, Stepanova M, Afendy M, et al. (2011) Changes in the prevalence of the most common causes of chronic liver diseases in the United States from 1988 to 2008. Clin Gastroenterol Hepatol 9:524–530
67. Williams CD, Stengel J, Asike MI, et al. (2011) Prevalence of nonalcoholic fatty liver disease and nonalcoholic steatohepatitis among a largely middle-aged population utilizing ultrasound and liver biopsy: a prospective study. Gastroenterology 140:124–131
68. Welsh JA, Karpen S, Vos MB (2013) Increasing prevalence of nonalcoholic fatty liver disease among United States adolescents, 1988–1994 to 2007–2010. J Pediatr 162(496–500):e491
69. Chen J, Talwalkar JA, Yin M, et al. (2011) Early detection of nonalcoholic steatohepatitis in patients with nonalcoholic fatty liver disease by using MR elastography. Radiology 259:749–756
70. Kim D, Kim WR, Talwalkar JA, Kim HJ, Ehman RL (2013) Advanced fibrosis in nonalcoholic fatty liver disease: noninvasive assessment with MR elastography. Radiology 268:411–419
71. Loomba R, Wolfson T, Ang B, et al. (2014) Magnetic resonance elastography predicts advanced fibrosis in patients with nonalcoholic fatty liver disease: a prospective study. Hepatology. doi:10.1002/hep.27362
72. Venkatesh SK, Reeder SB (2014) New and improved imaging modalities for NAFLD. Curr Hepatol Rep 13:88–96
73. Vizzutti F, Arena U, Romanelli RG, et al. (2007) Liver stiffness measurement predicts severe portal hypertension in patients with HCV-related cirrhosis. Hepatology 45:1290–1297
74. Lim JK, Groszmann RJ (2007) Transient elastography for diagnosis of portal hypertension in liver cirrhosis: is there still a role for hepatic venous pressure gradient measurement? Hepatology 45:1087–1090
75. Sun HY, Lee JM, Han JK, Choi BI (2014) Usefulness of MR elastography for predicting esophageal varices in cirrhotic patients. J Magn Reson Imaging 39:559–566
76. Talwalkar JA, Yin M, Venkatesh SK, et al. (2009) Feasibility of in vivo MR elastographic splenic stiffness measurements in the assessment of portal hypertension. Am J Roentgenol 193:122–127
77. Shin SU, Lee JM, Yu MH, et al. (2014) Prediction of esophageal varices in patients with cirrhosis: usefulness of three-dimensional MR elastography with echo-planar imaging technique. Radiology. doi:10.1148/radiol.14130916
78. Fleming KM, Aithal GP, Card TR, West J (2012) All-cause mortality in people with cirrhosis compared with the general population: a population-based cohort study. Liver Int 32:79–84
79. Singh S, Fujii LL, Murad MH, et al. (2013) Liver stiffness is associated with risk of decompensation, liver cancer, and death in

patients with chronic liver diseases: a systematic review and meta-analysis. Clin Gastroenterol Hepatol 11(1573–84):83
80. Asrani SK, Talwalkar JA, Kamath PS, et al. (2014) Role of magnetic resonance elastography in compensated and decompensated liver disease. J Hepatol 60:934–939
81. O'Brien MJ, Keating NM, Elderiny S, et al. (2000) An assessment of digital image analysis to measure fibrosis in liver biopsy specimens of patients with chronic hepatitis C. Am J Clin Pathol 114:712–718
82. Venkatesh S, Yin M, Glockner J, et al. (2008) MR elastography of liver tumors: preliminary results. AJR Am J Roentgenol 190:1534–1540
83. Garteiser P, Doblas S, Daire JL, et al. (2012) MR elastography of liver tumours: value of viscoelastic properties for tumour characterisation. Eur Radiol 22:2169–2177
84. Crespo S, Bridges M, Nakhleh R, et al. (2013) Non-invasive assessment of liver fibrosis using magnetic resonance elastography in liver transplant recipients with hepatitis C. Clin Transplant 27:652–658
85. Kamphues C, Klatt D, Bova R, et al. (2012) Viscoelasticity-based magnetic resonance elastography for the assessment of liver fibrosis in hepatitis C patients after liver transplantation. Rofo 184:1013–1019
86. Serai SD, Wallihan DB, Venkatesh SK, et al. (2014) Magnetic resonance elastography of the liver in patients status-post fontan procedure: feasibility and preliminary results. Congenit Heart Dis 9(1):7–14
87. Serai SD, Wallihan DB, Venkatesh SK, Ehman RL, Podberesky DJ (2013) MR Elastography of the liver in patietns status post Fontan procedure: a pilot investigation. In: Proceedings of 21st annual ISMRM conference (abstract 3361), Salt Lake City, Utah
88. Mariappan YK, Venkatesh SK, Glaser JK, McGee KP, Ehman RL (2013) MR Elastography of liver with iron overload: development, evaluation and preliminary clinical experience with improved spin echo and spin echo EPI sequences. In: Proceedings of 21st annual ISMRM conference (abstract 278), Salt Lake City, Utah
89. Mannelli L, Godfrey E, Joubert I, et al. (2010) MR elastography: spleen stiffness measurements in healthy volunteers-preliminary experience. Am J Roentgenol 195:387–392
90. Morisaka H, Motosugi U, Ichikawa S, et al. (2013) Association of splenic MR elastographic findings with gastroesophageal varices in patients with chronic liver disease. J Magn Reson Imaging. doi: 10.1002/jmri.24505
91. Nedredal GI, Yin M, McKenzie T, et al. (2011) Portal hypertension correlates with splenic stiffness as measured with MR elastography. J Magn Reson Imaging 34:79–8795
92. Ronot M, Lambert S, Elkrief L, et al. (2014) Assessment of portal hypertension and high-risk oesophageal varices with liver and spleen three-dimensional multifrequency MR elastography in liver cirrhosis. Eur Radiol 24:1394–1402
93. Yin M, Venkatesh SK, Grimm RC, Rossman PJ, Manduca A, Ehman RL (2008) Assessment of the pancreas with MR elastography. In: Proceedings of the international society for magnetic resonance in medicine, Toronto, Canada, (abstract 2627).
94. Venkatesh SK, Yin M, Grimm RC, Rossman P, Ehman RL (2008) MR elastography of the kidneys: preliminary results. In: 16th annual meeting ISMRM, Toronto, Canada, (abstract 461)
95. Lerman LO, Bentley MD, Bell MR, Rumberger JA, Romero JC (1990) Quantitation of the in vivo kidney volume with cine computed tomography. Invest Radiol 25:1206–1211
96. Warner L, Yin M, Glaser KJ, et al. (2011) Noninvasive in vivo assessment of renal tissue elasticity during graded renal ischemia using MR elastography. Invest Radiol 46:509–514
97. Gennisson JL, Grenier N, Combe C, Tanter M (2012) Supersonic shear wave elastography of in vivo pig kidney: influence of blood pressure, urinary pressure and tissue anisotropy. Ultrasound Med Biol 38:1559–1567
98. Grenier N, Poulain S, Lepreux S, et al. (2012) Quantitative elastography of renal transplants using supersonic shear imaging: a pilot study. Eur Radiol 22:2138–2146
99. Rouviere O, Souchon R, Pagnoux G, Menager J-M, Chapelon JY (2011) Magnetic resonance elastography of the kidneys: feasibility and reproducibility in young healthy adults. J Magn Reson Imaging 34:880–886
100. Streitberger KJ, Guo J, Tzschätzsch H, et al. (2014) High-resolution mechanical imaging of the kidney. J Biomech 47:639–644
101. Lee CU, Glockner JF, Glaser KJ, et al. (2012) MR elastography in renal transplant patients and correlation with renal allograft biopsy: a feasibility study. Acad Radiol 19:834–841
102. Venkatesh SK, Wang G, Thamboo TP, et al. (2012) MR elastography of renal transplants: correlating stiffness with interstitial fibrosis and tubular atrophy. In: Proceedings of 20th annual meeting ISMRM, Melbourne, Australia (abstract 4062)
103. Jiang X, Asbach P, Streitberger KJ, et al. (2014) In vivo high-resolution magnetic resonance elastography of the uterine corpus and cervix. Eur Radiol 24:3025–3033
104. Norian JM, Owen CM, Taboas J, et al. (2012) Characterization of tissue biomechanics and mechanical signaling in uterine leiomyoma. Matrix Biol 31:57–65
105. Stewart EA, Taran FA, Chen J, et al. (2011) Magnetic resonance elastography of uterine leiomyomas: a feasibility study. Fertil Steril 95:281–284
106. Hesley G, Gorny K, Woodrum D (2013) MRE following focused ultrasound treatment of uterine fibroids. In: Focused ultrasound therapy—2nd European symposium, Rome, Italy (abstract)
107. Arani A, Da Rosa M, Ramsay E, et al. (2013) Incorporating endorectal MR elastography into multi-parametric MRI for prostate cancer imaging: Initial feasibility in volunteers. J Magn Reson Imaging 38:1251–1260
108. Sahebjavaher RS, Baghani A, Honarvar M, Sinkus R, Salcudean SE (2013) Transperineal prostate MR elastography: initial in vivo results. Magn Reson Med 69:411–420